

CEM-GMsFEM for Poisson equations in heterogeneous perforated domains

Wei Xie¹, Yin Yang², Eric Chung³, and Yunqing Huang⁴

¹National Center for Applied Mathematics in Hunan, Xiangtan University, Xiangtan 411105, Hunan, China. xiew@smail.xtu.edu.cn

²School of Mathematics and Computational Science, Xiangtan University, Xiangtan 411105, Hunan, China yangyinxtu@xtu.edu.cn

³Department of Mathematics, The Chinese University of Hong Kong, Shatin, Hong Kong SAR, tschung@math.cuhk.edu.hk

⁴School of Mathematics and Computational Science, Xiangtan University, Xiangtan 411105, Hunan, China huangyq@xtu.edu.cn

Abstract

In this paper, we propose a novel multiscale model reduction strategy tailored to address the Poisson equation within heterogeneous perforated domains. The numerical simulation of this intricate problem is impeded by its multiscale characteristics, necessitating an exceptionally fine mesh to adequately capture all relevant details. To overcome the challenges inherent in the multiscale nature of the perforations, we introduce a coarse space constructed using the Constraint Energy Minimizing Generalized Multiscale Finite Element Method (CEM-GMsFEM). This involves constructing basis functions through a sequence of local energy minimization problems over eigenspaces containing localized information pertaining to the heterogeneities. Through our analysis, we demonstrate that the oversampling layers depend on the local eigenvalues, thereby implicating the local geometry as well. Additionally, we provide numerical examples to illustrate the efficacy of the proposed scheme.

1 Introduction

Among multiscale problems, the problems in perforated domains are of great interest to many applications. These problems are characterized by processes taking place in domains with multiple scales, such as the presence of inclusions within the domain. Applications of perforated domain problems span a wide range, including fluid flow in porous media, diffusion in perforated domains, and mechanical processes in hollow materials, among others. Typically, the interaction between physical processes and heterogeneous media gives rise to challenges in perforated domains.

Numerous model reduction techniques have been developed in the existing literature to enhance computational efficiency for problems involving perforations. For instance, numerical upscaling methods [22, 23, 33] derive upscaled models and solve resulting problems globally on coarse grids, significantly reducing computational costs. Additionally, various multiscale methods have been proposed for simulating such problems. Multiscale finite element methods (MsFEM) [24, 25] of Crouzeix–Raviart type have been developed for elliptic problems [26] and Stokes flows [28]. The

Heterogeneous Multiscale Method (HMM) [21, 31] discretizes elliptic problems with perforations on coarse grids. Moreover, generalized finite element methods based on the idea of localized orthogonal decomposition (LOD) [27, 20] have been proposed for elliptic problems [3].

Recently, the Generalized Multiscale Finite Element Method (GMsFEM) [15, 6] has emerged as a promising framework for systematically enriching coarse spaces and incorporating fine-scale information in the construction of these spaces. This approach offers a convincing strategy for solving problems posed in heterogeneous perforated domains, characterized by multiscale features in their solutions and necessitating sophisticated enrichment techniques. The fundamental concept of GMsFEM involves employing local snapshots to approximate the fine-scale solution space, followed by the identification of local multiscale spaces through carefully selected local spectral problems defined within the snapshot spaces. These spectral problems provide a systematic approach to identifying dominant modes in the snapshot spaces, which are then selected to form the local multiscale spaces. By judiciously choosing the snapshot space and the spectral problem, GMsFEM requires only a few basis functions per coarse region to achieve solutions with excellent accuracy. Previous works have successfully applied GMsFEM to various problems, including Darcy’s flow model, Stokes equations, coupled flow and transport, and others in heterogeneous domains [11, 12, 14, 13, 29].

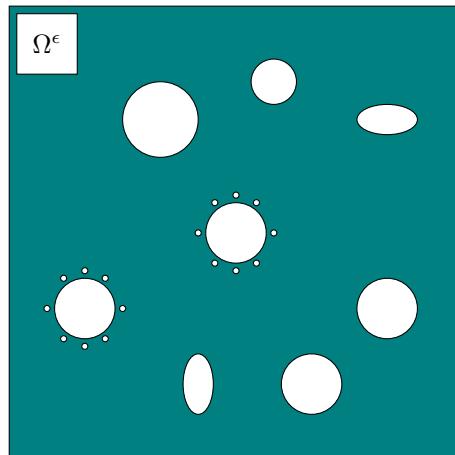


Figure 1: Illustration of a perforated domain.

In this work, we present a multiscale model reduction technique for Poisson equation in perforated domain (see Fig. 1). Our idea is motivated by the recently-developed Constraint Constraint Energy Minimizing Generalized Multiscale Finite Element Method (CEM-GMsFEM) [9, 10, 7]. This method has been applied successfully in dealing with many problems, e.g., poroelasticity problems [17, 16], quasi-gas problem [4], stokes problems in perforated domains [8], and others [5, 32, 30]. CEM-GMsFEM is based on the framework of GMsFEM to design multiscale basis functions such that the convergence of the method is independent of the contrast from the heterogeneities; and the error linearly decreases with respect to coarse mesh size if oversampling parameter is appropriately chosen. The multiscale basis functions in CEM-GMsFEM consists of two steps. One needs to first construct auxiliary basis functions by solving local spectral problems. Then, for each auxiliary basis function, one can construct a multiscale basis via energy minimization problems on an over-

sampling subdomains. We propose two versions, the first one is based on solving constraint energy minimization problems and the second one is the relax version by solving unconstrained energy minimization problems. In the following, we use constraint version for the former one while relaxed version to distinguish these two method. Consider the oversampling will lead extra computation, we will show the suitable oversampling layers depends on the eigenvalues of the local domain.

The paper is organized as follows. In Section 2, we present the model problem and the fine-scale approximation. In Section 3, we introduce auxiliary space and the construction of multiscale basis functions, both constraint version and relaxed version. Section 4 is devoted to analysis of the approach in Section 3 and show the decay is depends on the eigenvalues of the local domain. We will give some numerical results in Section 5 to show the efficiency of our proposed method. Conclusions will be included in Section 6.

2 Preliminaries

In this section, we state the Poisson equation in heterogeneous perforated domains and introduce some notations. Let $\Omega \subset \mathbb{R}^d (d = 2, 3)$ be a bounded domain. We set $\Omega^\epsilon \subset \Omega$ be a perforated domain and \mathcal{B}^ϵ be the perforations with Ω , that is $\Omega^\epsilon = \Omega \setminus \mathcal{B}^\epsilon$. The set of perforations \mathcal{B}^ϵ is assumed to be a union of connected circular disks, see Fig. 1 for illustration. Each of these disks is of diameter of order $0 < \epsilon \ll \text{diam}(\Omega)$. In perforated domain, we consider

$$\begin{cases} -\Delta u = f, & \text{in } \Omega^\epsilon, \\ \frac{\partial u}{\partial \mathbf{n}} = 0, & \text{on } \partial\Omega^\epsilon \cap \partial\mathcal{B}^\epsilon, \\ u = 0, & \text{on } \partial\Omega^\epsilon \cap \partial\Omega. \end{cases} \quad (1)$$

where \mathbf{n} stands for outward unit normal vectors to $\partial\Omega^\epsilon$. To define the weak formulation of (1), we introduce the space $V := \{v \in H^1(\Omega^\epsilon) : v|_{\partial\Omega^\epsilon \cap \partial\Omega} = 0\}$. The variational formulation of (1) is: Find $u \in V$, such that

$$a(u, v) = (f, v), \quad \forall v \in V, \quad (2)$$

where

$$a(u, v) = \int_{\Omega^\epsilon} \nabla u \nabla v, \quad (f, v) = \int_{\Omega^\epsilon} f v.$$

Let \mathcal{T}^h be a triangulation of perforated domain Ω^ϵ . In here, h is the triangle mesh size, we assume \mathcal{T}^h is sufficiently fine to fully resolve the small-scale information of the domain Ω^ϵ . We can define a finite space V_h via the linear basis functions on \mathcal{T}^h . The continuous Galerkin (CG) formulation of (1) is : Find $u_h \in V_h$, such that

$$a(u_h, v_h) = (f, v_h), \quad \forall v_h \in V_h. \quad (3)$$

Let φ_i to denote the linear basis functions in \mathcal{T}^h . Then, $V_h = \{\varphi_i\}_{i=1}^N$, where N is the interior nodes within the mesh \mathcal{T}^h and boundary nodes intersecting \mathcal{B}^ϵ . We do not need any hat functions on the boudary of Ω , because the functions in V_h must vanish here. Now, using this basis, we can conclude the finite element method (3) is equivalent to

$$a(u_h, \varphi_i) = (f, \varphi_i), \quad \forall \varphi_i \in V_h. \quad (4)$$

the equivalent matrix form of (4) is

$$Au_h = F \quad (5)$$

where

$$A_{ij} = a(\varphi_j, \varphi_i), \quad F_i = (f, \varphi_i).$$

In this paper, we will use a multiscale model reduction technique that construct a multiscale space V_{ms} to reduce the cost compare to (5). We have to point out that the multiscale space V_{ms} is a subset of V , that is $V_{\text{ms}} \subset V$. The multiscale solution is: Find $u_{\text{ms}} \in V_{\text{ms}}$ such that

$$a(u_{\text{ms}}, v) = (f, v), \quad \forall v \in V_{\text{ms}} \quad (6)$$

In the subsequent sections, we will still use the linear basis functions on \mathcal{T}^h to compute auxiliary space and multiscale space numerically. Then, each multiscale basis functions can be linear expressed by $\{\varphi_i\}$, using a discrete vector Ψ_j to denote the coefficient of j -th multiscale basis. We can define an upscaling matrix R^T that stores all the multiscale basis functions (total number is N_{ms}),

$$R^T = \begin{bmatrix} \Psi_1 & \Psi_2 & \cdots & \Psi_{N_{\text{ms}}} \end{bmatrix}$$

The construction of multiscale basis functions will be introduced in Section 3. Then, the coarse grid solution is $u_H = (R^T A R)^{-1} (R^T F)$, the multiscale solution need to multiply the downscaling matrix R , that is $u_{\text{ms}} = R^T u_H$.

3 The construction of the CEM-GMsFEM basis functions

In this section, we construct multiscale spaces on coarse grid. Let \mathcal{T}^H be a conforming partition of the computational domain Ω^ϵ , such that each element is the union of triangle in \mathcal{T}^h . Using H represent the coarse mesh size. Typically, we assume that $0 < h \ll H < \text{diam}(\Omega)$. Let N_c be the total number of coarse elements and N_v be the total number of vertices of \mathcal{T}^H .

The construction of the multiscale spaces consists of two steps. The first step is to construct auxiliary multiscale spaces which the concept is similar of GMsFEM, we will compute a eigenvalue problem in each coarse block K_i . Then, for each K_{i,m_i} that enlarging K_i by m_i coarse grid layers, we will solving the energy minimizing problems in the oversampled domains. In Fig. 2, we illustrates the fine-scale triangulation, coarse element K_i and oversampling subdomains $K_{i,1}$. If the parameter m_i is appropriately chosen, the error demonstrates linear convergence towards the reference solution in relation to the coarse mesh size H . This assertion is rigorously established and substantiated in the subsequent section.

3.1 Auxiliary space

We will construct the auxiliary multiscale basis functions in each coarse block K_i . Before started, we need define two inner product $a_i(\cdot, \cdot)$, $s_i(\cdot, \cdot)$ in K_i ,

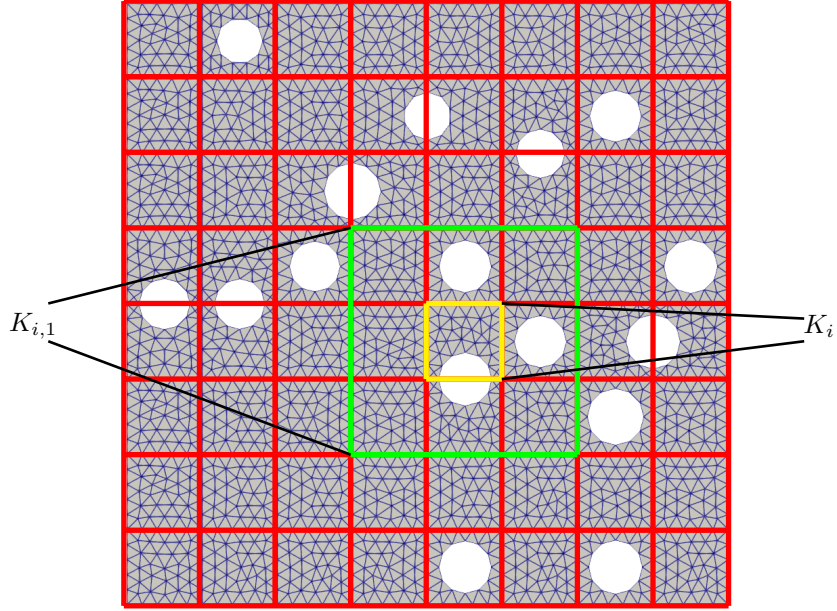


Figure 2: Illustration of the coarse grid (Red), the fine-grid (Blue) and the oversampling domain (Green).

$$a_i(v, w) = \int_{K_i} \nabla v \cdot \nabla w, \quad s_i(v, w) = \int_{K_i} \tilde{\kappa} v w. \quad (7)$$

where $\tilde{\kappa} = \sum_{j=1}^{N_v} |\nabla \chi_j|^2$ and $\{\chi_j\}_{j=1}^{N_v}$ are the partition of unity functions [2] that defined on coarse grid. In particular, the function χ_j satisfies $|\nabla \chi_j| = O(1/H)$ and $0 \leq \chi_j \leq 1$, we use the Lagrange basis for simplify computation in here. Consider the following local eigenvalue problem,

$$a_i(\phi_j^i, v) = \lambda_j^i s_i(\phi_j^i, v), \quad \forall v \in H^1(K_i). \quad (8)$$

Solving (8), arrange the eigenvalues in ascending order such that

$$0 = \lambda_1^i \leq \lambda_2^i \leq \dots \leq \lambda_{l_i}^i \leq \dots$$

for each $i \in \{1, 2, \dots, N_c\}$. We use the first l_i eigenfunctions to construct the local auxiliary space, $V_{\text{aux}}^i = \text{span}\{\phi_1^i, \dots, \phi_{l_i}^i\}$. We have to note that ϕ_j^i are a set of unit orthogonal functions with $s(\cdot, \cdot)$ inner product. Based on that, we can define the global auxiliary space $V_{\text{aux}} = \oplus_i V_{\text{aux}}^i$. Given a function $\phi_j^i \in V_{\text{aux}}$, we say that a function ψ is ϕ_j^i -orthogonal if

$$s(\psi, \phi_j^i) = 1, \quad s(\psi, \phi_{j'}^{i'}) = 0, \quad \text{if } j' \neq j \text{ or } i' \neq i.$$

where $s(u, v) = \sum_{i=1}^{N_c} s_i(u, v)$. We also define a global operator $\pi : V \rightarrow V_{\text{aux}}$,

$$\pi(u) = \sum_{i=1}^{N_c} \sum_{j=1}^{l_i} \frac{s_i(u, \phi_j^i)}{s_i(\phi_j^i, \phi_j^i)} \phi_j^i, \quad \forall u \in V.$$

In particular, we define \tilde{V} as the null space of the projection π , namely, $\tilde{V} = \{v \in V \mid \pi(v) = 0\}$.

3.2 Multiscale space

Similar to the previous work [9, 7], we can construct two different type of multiscale basis functions on a oversampling domain. But differently, we choose different oversampling layers for each coarse block with can gives more flexibility and save computations. For each coarse block K_i , we can extend this region by m_i coarse grid layer and obtain an oversampled region K_{i,m_i} (see Fig. 2). Then for each auxiliary function $\phi_j^i \in V_{\text{aux}}^i$, the multiscale basis function $\psi_{j,\text{ms}}^i$ can be defined by

$$\psi_{j,\text{ms}}^i = \operatorname{argmin}\{a(\psi, \psi) \mid \psi \in V_0(K_{i,m_i}), \psi \text{ is } \phi_j^i\text{-orthogonal}\} \quad (9)$$

where $V_0(K_{i,m_i}) = \{v \in H^1(K_{i,m_i}) \mid v = 0 \text{ in } \partial K_{i,m_i} / (\partial K_{i,m_i} \cap \partial \mathcal{B}^\epsilon)\}$. Refer to [18], by using Lagrange Multiplier, the problem (9) can be rewritten as the following problem: find an $(\psi_{j,\text{ms}}^i, w) \in V_0(K_{i,m_i}) \times V_{\text{aux}}(K_{i,m_i})$,

$$\begin{cases} a(\psi_{j,\text{ms}}^i, v) + s(v, w) = 0, & \forall v \in V_0(K_{i,m_i}), \\ s(\psi_{j,\text{ms}}^i - \phi_j^i, q) = 0, & \forall q \in V_{\text{aux}}(K_{i,m_i}). \end{cases} \quad (10)$$

where $V_{\text{aux}}(K_{i,m_i})$ is the union of all local auxiliary spaces for $K_j \subset K_{i,m_i}$. In fact, $\psi_{j,\text{ms}}^i$ can be numerically solved on the fine scale mesh. Besides, w belongs to auxiliary space, it can be expressed by ϕ_j^i . We using A^i, S^i to denote the stiff matrix and mass matrix in K_{i,m_i} that defined by inner product in (7). The column of matrix P^i is the discrete style of all auxiliary basis function includes in $V_{\text{aux}}(K_{i,m_i})$, the matrix form of (10) is,

$$\begin{bmatrix} A^i & S^i P^i \\ (S^i P^i)^T & \mathbf{0} \end{bmatrix} \begin{bmatrix} \psi_h^i \\ w_h \end{bmatrix} = \begin{bmatrix} \mathbf{0} \\ I \end{bmatrix} \quad (11)$$

where I is a sparse matrix whose nonzero elements (all are 1) depends on the index order of the corresponding auxiliary basis function ϕ_j^i in $V_{\text{aux}}(K_{i,m_i})$. For our convergence analysis, we need to define a global basis functions. The global multiscale basis function of constraint version is $\psi_j^i \in V$ is defined in a similar way, namely,

$$\psi_j^i = \operatorname{argmin}\{a(\psi, \psi) \mid \psi \in V, \psi \text{ is } \phi_j^i\text{-orthogonal}\}. \quad (12)$$

We can also get the equivalent variational problem,

$$\begin{cases} a(\psi_j^i, v) + s(v, w) = 0, & \forall v \in V, \\ s(\psi_j^i - \phi_j^i, q) = 0, & \forall q \in V_{\text{aux}}. \end{cases} \quad (13)$$

Following [9], we can relax the ϕ -orthogonality in (9) and get a relaxed version of the multiscale basis functions. More specifically, we solve the following un-constrained minimization problem: Find $\psi_{j,\text{ms}}^i \in V_0(K_{i,m_i})$ such that

$$\psi_{j,\text{ms}}^i = \operatorname{argmin}\{a(\psi, \psi) + s(\pi(\psi) - \phi_j^i, \pi(\psi) - \phi_j^i) \mid \psi \in V_0(K_{i,m_i})\}. \quad (14)$$

we can also derive the variation form of (14),

$$a(\psi_{j,\text{ms}}^i, v) + s(\pi(\psi_{j,\text{ms}}^i), \pi(v)) = s(\phi_j^i, \pi(v)), \quad \forall v \in V_0(K_{i,m_i}). \quad (15)$$

Using the same notation before, the matrix form of (15) is,

$$(A^i + (S^i P^i)(S^i P^i)^T) \psi_{j,h}^i = P_j^i S^{i,T} \quad (16)$$

where P_j^i is the j -th eigenfunction in V_{aux}^i . The relaxed version of global multiscale basis function $\psi_j^i \in V$ is defined in a similar way, namely,

$$\psi_j^i = \operatorname{argmin}\{a(\psi, \psi) + s(\pi(\psi) - \phi_j^i, \pi(\psi) - \phi_j^i) \mid \psi \in V\}. \quad (17)$$

which is equivalent to the following variational form

$$a(\psi_j^i, v) + s(\pi(\psi_j^i), \pi(v)) = s(\phi_j^i, \pi(v)), \quad \forall v \in V. \quad (18)$$

We have to note that multiscale basis functions $\psi_{j,\text{ms}}^i$ is corresponding to auxiliary basis ϕ_j^i one by one both for constraint version and relaxed version. After we construct multiscale basis functions for each K_{i,m_i} , we can define the multiscale space,

$$V_{\text{ms}} = \operatorname{span}\{\psi_{j,\text{ms}}^i \mid 1 \leq j \leq l_i, 1 \leq i \leq N_c\}.$$

Then the multiscale approximation is

$$a(u_{\text{ms}}, v) = (f, v), \quad \forall v \in V_{\text{ms}}. \quad (19)$$

Through this two different type of global multiscale basis function, we can also define V_{glo} is

$$V_{\text{glo}} = \operatorname{span}\{\psi_j^i \mid 1 \leq j \leq l_i, 1 \leq i \leq N_c\}.$$

Then the global approximation is

$$a(u_{\text{glo}}, v) = (f, v), \quad \forall v \in V_{\text{glo}}. \quad (20)$$

This global multiscale finite element space V_{glo} satisfies a very important orthogonality property, which will be used in our convergence analysis. Recall \tilde{V} is the null space of projection π , for any $v \in \tilde{V}$, constraint version and relaxed version of global multiscale basis function ψ_j^i can conclude, $a(\psi_j^i, v) = 0$, which is obviously in (13) and (18). Therefore, we have $\tilde{V} \subset V_{\text{glo}}^\perp$. Since $\dim(V_{\text{glo}}) = \dim(V_{\text{aux}})$, we have $\tilde{V} = V_{\text{glo}}^\perp$. Thus, we can conclude $V = V_{\text{glo}} \oplus \tilde{V}$.

4 Convergence analysis

In this section, we establish the convergence of the method introduced in Section 3. Before proving the convergence of the method, we need to define some notations and some lemma that suitable for both constraint version and relaxed version. We will define three different norms. The first norm is L^2 -norm $\|\cdot\|$ where $\|u\| = \int_{\Omega^\epsilon} u^2$. Second is the a -norm $\|\cdot\|_a$ where $\|u\|_a^2 = \int_{\Omega^\epsilon} |\nabla u|^2$, while the last is s -norm $\|\cdot\|_s$ where $\|u\|_s^2 = \int_{\Omega^\epsilon} \tilde{\kappa} u^2$. For a given subdomain $\omega \subset \Omega^\epsilon$, we will define the local a -norm and s -norm by $\|u\|_{a(\omega)}^2 = \int_\omega |\nabla u|^2$ and $\|u\|_{s(\omega)}^2 = \int_\omega \tilde{\kappa} u^2$.

In this work, we need to define Λ, Γ as the following.

$$\Lambda_\omega = \min_{K_i \cap \omega \neq \emptyset} \lambda_{l_i+1}^i, \quad \Gamma_\omega = \max_{K_i \cap \omega \neq \emptyset} \lambda_{l_i}^i,$$

where ω is a subset of Ω^ϵ . Similiar with [9, 8], we need the cutoff function to estimate the difference between the global and multiscale basis function. For each K_i , consider that $K_{i,m_i} \subset \Omega^\epsilon$ denotes the oversampling coarse region obtained by enlarging K_i with m_i additional coarse layers. For $M_i > m_i$, we define $\chi_i^{M_i, m_i} \in \text{span}\{\chi_j\}_{j=1}^{N_v}$ such that $0 \leq \chi_i^{M_i, m_i} \leq 1$ and

$$\chi_i^{M_i, m_i} = \begin{cases} 1 & \text{in } K_{i, m_i}, \\ 0 & \text{in } \Omega^\epsilon \setminus K_{i, M_i}. \end{cases} \quad (21)$$

Note that, we have $K_{i, m_i} \subset K_{i, M_i} \subset \Omega^\epsilon$. The prove is very similar to the previous work [9, 8], but we will prove the oversampling layers k_i is also dependent of the eigenvalues in the oversampling domain, and define $k = \max_{1 \leq i \leq N_c} k_i$. Before analyse the multiscale solution, we need some estimate between different norms for later use in the analysis.

Lemma 1. *Let $k_i \geq 2$ be an integer and define $W := \{v \in V \mid v|_{K_i} \notin V_{\text{aux}}^i\}$. Then, the following inequalities hold*

(i) if $v \in V_{\text{aux}}^i$, $\|v\|_{a(K_i)}^2 \leq \lambda_{l_i}^i \|v\|_{s(K_i)}^2$.

(ii) if $v \in W$, $\|v\|_s^2 \leq \Lambda_{\text{supp}(v)}^{-1} \|v\|_a^2$.

(iii) if $v \in V$, $\|v\|_s^2 \leq \Lambda_{\text{supp}(v)}^{-1} \|(I - \pi)v\|_a^2 + \|\pi(v)\|_s^2$.

(iv) if $v \in V$,

$$\|(1 - \chi_i^{k_i, k_i-1})v\|_a^2 \leq 2(1 + \Lambda_{\text{supp}(v)}^{-1}) \|v\|_{a(\Omega^\epsilon \setminus K_{i, k_i-1})}^2 + 2\|\pi(v)\|_{s(\Omega^\epsilon \setminus K_{i, k_i-1})}^2$$

(v) if $v \in V$, $\|(1 - \chi_i^{k_i, k_i-1})v\|_s^2 \leq \Lambda_{\text{supp}(v)}^{-1} \|v\|_{a(\Omega^\epsilon \setminus K_{i, k_i-1})}^2 + \|\pi(v)\|_{s(\Omega^\epsilon \setminus K_{i, k_i-1})}^2$.

Proof. For any $z \in H^1(K_i)$, we can present $z = \sum_{j \geq 1} \alpha_j^i \phi_j^i$ with $\alpha_j^i \in \mathbb{R}$.

(i) Since $v \in V_{\text{aux}}^i$, then $\alpha_j^i = 0$ for $j \geq l_i + 1$. Recall the eigenfunctions that using local spectral problem (8) are orthogonal to each other, we obtain

$$\|v\|_{a(K_i)}^2 = \sum_{j=1}^{l_i} \alpha_j^i \lambda_j^i s(\phi_j^i, v) \leq \lambda_{l_i}^i \sum_{j=1}^{l_i} \alpha_j^i s(\phi_j^i, v) = \lambda_{l_i}^i \|v\|_{s(K_i)}^2.$$

(ii) For any $v \in W$, then $v = \sum_{i=1}^{N_c} \sum_{j \geq l_i+1} \alpha_j^i \phi_j^i$.

$$\begin{aligned}
\|v\|_a^2 &= \sum_{K_i \subset \text{supp}(v)} \sum_{j \geq l_i+1} \alpha_j^i a_i(\phi_j^i, v) \\
&= \sum_{K_i \subset \text{supp}(v)} \sum_{j \geq l_i+1} \alpha_j^i \lambda_j^i s_i(\phi_j^i, v) \\
&\geq \Lambda_{\text{supp}(v)} \sum_{i=1}^{N_c} \sum_{j \geq l_i+1} \alpha_j^i s(\phi_j^i, v) \\
&= \Lambda_{\text{supp}(v)} \|v\|_s^2.
\end{aligned}$$

(iii) For any $v \in V$,

$$\begin{aligned}
\|v\|_s^2 &\leq \|(I - \pi)v\|_s^2 + \|\pi(v)\|_s^2 \\
&\leq \Lambda_{\text{supp}(v)}^{-1} \|(I - \pi)v\|_a^2 + \|\pi(v)\|_s^2.
\end{aligned}$$

where operator I means the identity operator, the last inequality is follows from (ii).

(iv) By using the property of cutoff function $\chi_i^{k_i, k_i-1}$ and (iii),

$$\begin{aligned}
&\|(1 - \chi_i^{k_i, k_i-1})v\|_a^2 \\
&= \int_{\Omega^\epsilon \setminus K_{i, k_i-1}} \left| \nabla \left((1 - \chi_i^{k_i, k_i-1})v \right) \right|^2 \\
&\leq 2 \int_{\Omega^\epsilon \setminus K_{i, k_i-1}} (1 - \chi_i^{k_i, k_i-1})^2 |\nabla v|^2 + |v \nabla \chi_i^{k_i, k_i-1}|^2 \\
&\leq 2(\|v\|_{a(\Omega^\epsilon \setminus K_{i, k_i-1})}^2 + \|v\|_{s(\Omega^\epsilon \setminus K_{i, k_i-1})}^2) \\
&\leq 2(1 + \Lambda_{\Omega^\epsilon \setminus K_{i, k_i-1}}^{-1}) \|v\|_{a(\Omega^\epsilon \setminus K_{i, k_i-1})}^2 + 2\|\pi(v)\|_{s(\Omega^\epsilon \setminus K_{i, k_i-1})}^2
\end{aligned}$$

(v) For any $k_i \geq 2$ and combine (iii), we have

$$\begin{aligned}
\|(1 - \chi_i^{k_i, k_i-1})v\|_s^2 &\leq \|v\|_{s(\Omega^\epsilon \setminus K_{i, k_i-1})}^2 \\
&\leq \Lambda_{\Omega^\epsilon \setminus K_{i, k_i-1}}^{-1} \|v\|_{a(\Omega^\epsilon \setminus K_{i, k_i-1})}^2 + \|\pi(v)\|_{s(\Omega^\epsilon \setminus K_{i, k_i-1})}^2.
\end{aligned}$$

This completes the proof. \square

To prove the convergence result of the proposed method, we need to recall the convergence result of using the global multiscale basis functions in [9].

Lemma 2. *Let u be the solution of (2) and u_{glo} be the solution of (20). We have*

$$\|u - u_{\text{glo}}\|_a \leq C \Lambda_{\Omega^\epsilon}^{-\frac{1}{2}} \|\tilde{\kappa}^{-\frac{1}{2}} f\|.$$

Moreover, if $\{\chi_j\}_{j=1}^{N_c}$ is a set of bilinear partition of unity, we have

$$\|u - u_{\text{glo}}\|_a \leq CH \Lambda_{\Omega^\epsilon}^{-\frac{1}{2}} \|f\|.$$

To achieve convergence, we must assess the disparity between global and local multiscale basis functions. Given the distinct construction methods of constraint version and relaxed version, separate estimations are necessary. The estimation of the distinction between global and multiscale basis functions relies on a lemma applicable to both versions of multiscale basis functions. For each coarse block K , we define B as a bubble function with $B(\mathbf{x}) > 0$ for all $\mathbf{x} \in K$ and $B(\mathbf{x}) = 0$ for all $\mathbf{x} \in \partial K$. We will take $B = \prod_j \chi_j$ where the product is taken over all vertices j on the boundary of K . Using the bubble function, we define the constant

$$C_\pi = \sup_{K \in \mathcal{T}^H, \mu \in V_{\text{aux}}} \frac{\int_K \tilde{\kappa} \mu^2}{\int_K B \tilde{\kappa} \mu^2}.$$

Lemma 3. *For all $v_{\text{aux}} \in V_{\text{aux}}$, there exists a function $v \in V$ such that*

$$\pi(v) = v_{\text{aux}}, \quad \|v\|_a^2 \leq D_{\text{supp}(v)} \|v_{\text{aux}}\|_s^2, \quad \text{supp}(v) \subset \text{supp}(v_{\text{aux}}),$$

where $D_{\text{supp}(v)} = C_{\mathcal{T}}(1 + \Gamma_{\text{supp}(v)})$, and $C_{\mathcal{T}}$ is the square of the maximum number of vertices over all coarse elements.

Proof. Without loss of generality, we can assume that $v_{\text{aux}} \in V_{\text{aux}}^i$. Consider the following variational problem: find $v \in V(K_i)$ and $\mu \in V_{\text{aux}}^i$ such that

$$\begin{cases} a_i(v, w) + s_i(w, \mu) = 0, & \forall w \in V(K_i), \\ s_i(v - v_{\text{aux}}, q) = 0, & \forall q \in V_{\text{aux}}^i. \end{cases} \quad (22)$$

Note that, the well-posedness of the problem (22) is equivalent to the existence of a function $v \in V(K_i)$ such that

$$s_i(v, v_{\text{aux}}) \geq C_1 \|v_{\text{aux}}\|_{s(K_i)}^2, \quad \|v\|_{a(K_i)} \leq C_2 \|v_{\text{aux}}\|_{s(K_i)}$$

where C_1 and C_2 are the constants to be determined.

Note that v_{aux} is supported in K_i . We let $v = Bv_{\text{aux}}$. By the definition of s_i , we have

$$s_i(v, v_{\text{aux}}) = \int_{K_i} \tilde{\kappa} B v_{\text{aux}}^2 \geq C_\pi^{-1} \|v_{\text{aux}}\|_{s(K_i)}^2.$$

Since $\nabla(Bv_{\text{aux}}) = v_{\text{aux}} \nabla B + B \nabla v_{\text{aux}}$, $|B| \leq 1$ and $|\nabla B|^2 \leq C_{\mathcal{T}} \sum_j |\nabla \chi_j|^2$, we have

$$\|v\|_{a(K_i)}^2 = a_i(v, Bv_{\text{aux}}) \leq C_{\mathcal{T}} \|v\|_{a(K_i)} (\|v_{\text{aux}}\|_{a(K_i)} + \|v_{\text{aux}}\|_{s(K_i)}).$$

Combining lemma 1 (i), the existence and uniqueness of the function v can be deduced for a given auxiliary function $v_{\text{aux}} \in V_{\text{aux}}^i$. It is evident from the second equality in (22) that $\pi(v) = v_{\text{aux}}$. The remaining two conditions in the lemma naturally follow from the preceding proof. It is important to note that the constant D depends on the eigenvalues that in support of v_{aux} . \square

Next, we will separately establish the remaining components of the convergence analysis for both the constraint version and the relaxed version. That is, our goal is to estimate the difference of multiscale basis functions and global multiscale basis functions.

4.1 Constraint Version

Before we start analyze the constraint version, we need to estimate the difference of multiscale basis functions and global multiscale basis functions are dependent of the oversampling layers. The following lemma has prove the exponential decay property.

Lemma 4. *We consider the oversampled domain K_{i,k_i} with $k_i \geq 2$. That is, K_{i,k_i} is an oversampled region by enlarging K_i by k_i coarse grid layers. Let $\phi_j^i \in V_{\text{aux}}$ be a given auxiliary multiscale basis function. We let $\psi_{j,\text{ms}}^i$ be the multiscale basis functions obtained in (9) and let ψ_j^i be the global multiscale basis functions obtained in (12). Then we have*

$$\|\psi_j^i - \psi_{j,\text{ms}}^i\|_a^2 \leq E_i \|\phi_j^i\|_{s(K_i)}^2$$

$$\text{where } E_i = 8D_{K_{i,k_i}}^2 (1 + \Lambda_{\Omega^\epsilon \setminus K_{i,k_i}}^{-1}) \left(1 + \frac{\Lambda_{K_{i,k_i-1}}^{\frac{1}{2}}}{2D_{K_{i,k_i-1}}^{\frac{1}{2}}}\right)^{1-k_i}.$$

Proof. For the given $\phi_j^i \in V_{\text{aux}}$, using lemma 3, there exists a $\tilde{\phi}_j^i \in V$ such that

$$\pi(\tilde{\phi}_j^i) = \phi_j^i, \quad \|\tilde{\phi}_j^i\|_a^2 \leq D_{K_i} \|\phi_j^i\|_{s(K_i)}^2, \quad \text{and} \quad \text{supp}(\tilde{\phi}_j^i) \subset K_i. \quad (23)$$

We let $\eta = \psi_j^i - \tilde{\phi}_j^i$. Note that $\eta \in \tilde{V}$ since $\pi(\eta) = 0$. By using the resulting variational forms of minimization problems (9) and (12), we see that $\psi_{j,\text{ms}}^i$ and ψ_j^i satisfy

$$a(\psi_{j,\text{ms}}^i, v) + s(v, \mu_{j,\text{ms}}^i) = 0, \quad \forall v \in V_0(K_{i,k_i}) \quad (24)$$

where $V_0(K_{i,k_i}) = \{v \in H^1(K_{i,k_i}) \mid v = 0 \text{ in } \partial K_{i,k_i} / (\partial K_{i,k_i} \cap \partial \mathcal{B}^\epsilon)\}$, and

$$a(\psi_j^i, v) + s(v, \mu_j^i) = 0, \quad \forall v \in V \quad (25)$$

for some $\mu_{j,\text{ms}}^i, \mu_j^i \in V_{\text{aux}}$. Define a null space in K_{i,k_i} ,

$$\tilde{V}_0(K_{i,k_i}) = \{v \in V_0(K_{i,k_i}) \mid \pi(v) = 0\}.$$

Subtracting the above two equations (24) and (25), and restricting $v \in \tilde{V}_0(K_{i,k_i})$, we have

$$a(\psi_j^i - \psi_{j,\text{ms}}^i, v) = 0, \quad \forall v \in \tilde{V}_0(K_{i,k_i}).$$

Therefore, for $v \in \tilde{V}_0(K_{i,k_i})$ and combine $(-\psi_{j,\text{ms}}^i + \tilde{\phi}_j^i) \in \tilde{V}(K_{i,k_i})$, we have

$$\begin{aligned} \|\psi_j^i - \psi_{j,\text{ms}}^i\|_a^2 &= a(\psi_j^i - \psi_{j,\text{ms}}^i, \psi_j^i - \psi_{j,\text{ms}}^i) \\ &= a(\psi_j^i - \psi_{j,\text{ms}}^i, \psi_j^i - \tilde{\phi}_j^i - \psi_{j,\text{ms}}^i + \tilde{\phi}_j^i) \\ &= a(\psi_j^i - \psi_{j,\text{ms}}^i, \eta - v). \end{aligned}$$

Hence, we conclude

$$\|\psi_j^i - \psi_{j,\text{ms}}^i\|_a \leq \|\eta - v\|_a \quad (26)$$

for all $v \in \tilde{V}_0(K_{i,k_i})$. For i -th coarse block K_i , we consider two oversampled regions K_{i,k_i-1} and K_{i,k_i} . We define the cutoff function $\chi_i^{k_i,k_i-1}$ with the properties in (21), where $M_i = k_i$ and $m_i = k_i - 1$. It follows that $\chi_i^{k_i,k_i-1} \equiv 1$ for any $K_j \subset K_{i,k_i-1}$. Since $\eta \in \tilde{V}$, we have

$$s_j(\chi_i^{k_i,k_i-1}\eta, \phi_n^j) = s_j(\eta, \phi_n^j) = 0, \quad \forall n = 1, 2, \dots, l_j.$$

From the above result and the fact that $\chi_i^{k_i,k_i-1} \equiv 0$ in $\Omega^\epsilon \setminus K_{i,k_i}$, we have

$$\text{supp} \left(\pi(\chi_i^{k_i,k_i-1}\eta) \right) \subset K_{i,k_i} \setminus K_{i,k_i-1}.$$

Using lemma 3, for the function $\pi(\chi_i^{k_i,k_i-1}\eta)$, there is $\mu \in V$ such that $\text{supp}(\mu) \subset K_{i,k_i} \setminus K_{i,k_i-1}$ and $\pi(\mu - \chi_i^{k_i,k_i-1}\eta) = 0$. Moreover, also from lemma 3,

$$\begin{aligned} \|\mu\|_{a(K_{i,k_i} \setminus K_{i,k_i-1})} &\leq D_{K_{i,k_i} \setminus K_{i,k_i-1}}^{\frac{1}{2}} \|\pi(\chi_i^{k_i,k_i-1}\eta)\|_{s(K_{i,k_i} \setminus K_{i,k_i-1})} \\ &\leq D_{K_{i,k_i} \setminus K_{i,k_i-1}}^{\frac{1}{2}} \|\chi_i^{k_i,k_i-1}\eta\|_{s(K_{i,k_i} \setminus K_{i,k_i-1})} \end{aligned} \quad (27)$$

where the last inequality follows from the fact that π is a projection. Taking $v = \mu + \chi_i^{k_i,k_i-1}\eta$ in (26), we have

$$\|\psi_j^i - \psi_{j,\text{ms}}^i\|_a \leq \|\eta - v\|_a \leq \|(1 - \chi_i^{k_i,k_i-1})\eta\|_a + \|\mu\|_{a(K_{i,k_i} \setminus K_{i,k_i-1})}. \quad (28)$$

Next, we will use three steps to estimate the two terms on the right hand side.

Step 1: We will prove the two terms on the right hand side in (28) can be bounded by $\|\eta\|_{a(\Omega^\epsilon \setminus K_{i,k_i-1})}$. For the first term in (28), $\|(1 - \chi_i^{k_i,k_i-1})\eta\|_a$. From lemma 1 (iv) and $\eta \in \tilde{V}$, we have

$$\|(1 - \chi_i^{k_i,k_i-1})\eta\|_a^2 \leq 2(1 + \Lambda_{\Omega^\epsilon \setminus K_{i,k_i-1}}^{-1}) \|\eta\|_{a(\Omega^\epsilon \setminus K_{i,k_i-1})}^2.$$

For the second term in (28), $\|\mu\|_{a(K_{i,k_i} \setminus K_{i,k_i-1})}$. By (27) and lemma 1 (ii), we have

$$\begin{aligned} \|\mu\|_{a(K_{i,k_i} \setminus K_{i,k_i-1})}^2 &\leq D_{K_{i,k_i} \setminus K_{i,k_i-1}} \|\chi_i^{k_i,k_i-1}\eta\|_{s(K_{i,k_i} \setminus K_{i,k_i-1})}^2 \\ &\leq \frac{D_{K_{i,k_i} \setminus K_{i,k_i-1}}}{\Lambda_{K_{i,k_i} \setminus K_{i,k_i-1}}} \|\eta\|_{a(K_{i,k_i} \setminus K_{i,k_i-1})}^2. \end{aligned}$$

Thus, we obtain

$$\|\psi_j^i - \psi_{j,\text{ms}}^i\|_a^2 \leq 2D_{K_{i,k_i} \setminus K_{i,k_i-1}} (1 + \Lambda_{\Omega^\epsilon \setminus K_{i,k_i-1}}^{-1}) \|\eta\|_{a(\Omega^\epsilon \setminus K_{i,k_i-1})}^2. \quad (29)$$

Step 2: We will prove the following recursive inequality,

$$\|\eta\|_{a(\Omega^\epsilon \setminus K_{i,k_i-1})}^2 \leq \left(1 + \frac{\Lambda_{K_{i,k_i-1} \setminus K_{i,k_i-2}}^{\frac{1}{2}}}{2D_{K_{i,k_i-1} \setminus K_{i,k_i-2}}} \right)^{-1} \|\eta\|_{a(\Omega^\epsilon \setminus K_{i,k_i-2})}^2. \quad (30)$$

where $k_i - 2 \geq 0$. Let $\xi = 1 - \chi_i^{k_i-1,k_i-2}$. Then we see that $\xi \equiv 1$ in $\Omega^\epsilon \setminus K_{i,k_i-1}$ and $0 \leq \xi \leq 1$ otherwise. Then we have

$$\|\eta\|_{a(\Omega^\epsilon \setminus K_{i,k_i-1})}^2 \leq \int_{\Omega^\epsilon} \xi^2 |\nabla \eta|^2 = \int_{\Omega^\epsilon} \nabla \eta \cdot \nabla (\xi^2 \eta) - 2 \int_{\Omega^\epsilon} \xi \eta \nabla \xi \cdot \eta. \quad (31)$$

We estimate the first term in (31). For the function $\pi(\xi^2 \eta)$, using lemma 3, there exist $\gamma \in V$ such that $\pi(\gamma) = \pi(\xi^2 \eta)$ and $\text{supp}(\gamma) \subset \text{supp}(\pi(\xi^2 \eta))$. For any coarse element $K_m \subset \Omega^\epsilon \setminus K_{i,k_i-1}$, since $\xi \equiv 1$ on K_m , we have

$$s_m(\xi^2 \eta, \phi_n^m) = 0, \quad \forall n = 1, 2, \dots, l_m.$$

On the other hand, since $\xi \equiv 0$ in K_{i,k_i-2} . For any coarse element $K_m \subset K_{i,k_i-2}$, we have

$$s_m(\xi^2 \eta, \phi_n^m) = 0, \quad \forall n = 1, 2, \dots, l_m.$$

From the above two conditions, we see that $\text{supp}(\pi(\xi^2 \eta)) \subset K_{i,k_i-1} \setminus K_{i,k_i-2}$, and consequently $\text{supp}(\pi(\gamma)) \subset K_{i,k_i-1} \setminus K_{i,k_i-2}$. Note that, since $\pi(\gamma) = \pi(\xi^2 \eta)$, we have $\xi^2 \eta - \gamma \in \tilde{V}$. We note also that $\text{supp}(\xi^2 \eta - \gamma) \subset \Omega^\epsilon \setminus K_{i,k_i-2}$. By (23), the functions $\tilde{\phi}_j^i$ and $\xi^2 \eta - \gamma$ have disjoint supports, so $a(\tilde{\phi}_j^i, \xi^2 \eta - \gamma) = 0$. Then, by the definition of η , we have

$$a(\eta, \xi^2 \eta - \gamma) = a(\psi_j^i, \xi^2 \eta - \gamma).$$

Since $\xi^2 \eta - \gamma \in \tilde{V} = V_{\text{glo}}^\perp$, we have $a(\psi_j^i, \xi^2 \eta - \gamma) = 0$. Then we can estimate the first term in (31) as follows

$$\begin{aligned} \int_{\Omega^\epsilon} \nabla \eta \cdot \nabla (\xi^2 \eta) &= \int_{\Omega^\epsilon} \nabla \eta \cdot \nabla \gamma \\ &\leq D_{K_{i,k_i-1} \setminus K_{i,k_i-2}}^{\frac{1}{2}} \|\eta\|_{a(K_{i,k_i-1} \setminus K_{i,k_i-2})} \|\pi(\xi^2 \eta)\|_{s(K_{i,k_i-1} \setminus K_{i,k_i-2})} \end{aligned}$$

where the last inequality follows from lemma 3. For all coarse elements $K_j \subset K_{i,k_i-1} \setminus K_{i,k_i-2}$, since $\pi(\eta) = 0$, combine lemma 1 (ii), we have

$$\|\pi(\xi^2 \eta)\|_{s(K_j)}^2 \leq \|\xi^2 \eta\|_{s(K_j)}^2 \leq \Lambda_{K_j}^{-1} \|\eta\|_{a(K_j)}^2.$$

Summing the above over all coarse elements $K_j \subset K_{i,k_i-1} \setminus K_{i,k_i-2}$, we have

$$\|\pi(\xi^2 \eta)\|_{s(K_{i,k_i-1} \setminus K_{i,k_i-2})} \leq \Lambda_{K_{i,k_i-1} \setminus K_{i,k_i-2}}^{-\frac{1}{2}} \|\eta\|_{a(K_{i,k_i-1} \setminus K_{i,k_i-2})}.$$

To estimate the second term in (31), using triangle inequality and lemma 1 (ii),

$$\begin{aligned} 2 \int_{\Omega^\epsilon} \xi \eta \nabla \xi \cdot \nabla \eta &\leq 2 \|\eta\|_{s(K_{i,k_i-1} \setminus K_{i,k_i-2})} \|\eta\|_{a(K_{i,k_i-1} \setminus K_{i,k_i-2})} \\ &\leq \Lambda_{K_{i,k_i-1} \setminus K_{i,k_i-2}}^{-\frac{1}{2}} \|\eta\|_{a(K_{i,k_i-1} \setminus K_{i,k_i-2})}^2. \end{aligned}$$

Hence, by using the above results, (31) can be estimated as

$$\|\eta\|_{a(\Omega^\epsilon \setminus K_{i,k_i-1})}^2 \leq \frac{2D_{K_{i,k_i-1} \setminus K_{i,k_i-2}}^{\frac{1}{2}}}{\Lambda_{K_{i,k_i-1} \setminus K_{i,k_i-2}}^{\frac{1}{2}}} \|\eta\|_{a(K_{i,k_i-1} \setminus K_{i,k_i-2})}^2.$$

By using the above inequality, we have

$$\begin{aligned}
\|\eta\|_{a(\Omega^\epsilon \setminus K_{i,k_i-2})}^2 &= \|\eta\|_{a(\Omega^\epsilon \setminus K_{i,k_i-1})}^2 + \|\eta\|_{a(K_{i,k_i-1} \setminus K_{i,k_i-2})}^2 \\
&\geq \left(1 + \frac{\Lambda_{K_{i,k_i-1} \setminus K_{i,k_i-2}}^{\frac{1}{2}}}{2D_{K_{i,k_i-1} \setminus K_{i,k_i-2}}^{\frac{1}{2}}}\right) \|\eta\|_{a(\Omega^\epsilon \setminus K_{i,k_i-1})}^2
\end{aligned}$$

Step 3: Finally, we will estimate the term $\|\eta\|_{a(\Omega^\epsilon \setminus K_{i,k_i-1})}$. Using (29) and (30), we conclude that

$$\begin{aligned}
&\|\psi_j^i - \psi_{j,\text{ms}}^i\|_a^2 \\
&\leq 2D_{K_{i,k_i} \setminus K_{i,k_i-1}} (1 + \Lambda_{\Omega^\epsilon \setminus K_{i,k_i-1}}^{-1}) \left(1 + \frac{\Lambda_{K_{i,k_i-1}}^{\frac{1}{2}}}{2D_{K_{i,k_i-1}}^{\frac{1}{2}}}\right)^{-1} \|\eta\|_{a(\Omega^\epsilon \setminus K_{i,k_i-2})}^2 \\
&\leq 2D_{K_{i,k_i} \setminus K_{i,k_i-1}} (1 + \Lambda_{\Omega^\epsilon \setminus K_{i,k_i-1}}^{-1}) \left(1 + \frac{\Lambda_{K_{i,k_i-1}}^{\frac{1}{2}}}{2D_{K_{i,k_i-1}}^{\frac{1}{2}}}\right)^{1-k_i} \|\eta\|_a^2.
\end{aligned} \tag{32}$$

By (23) and the definition of ψ_j^i , we have

$$\|\eta\|_a = \|\psi_j^i - \tilde{\phi}_j^i\|_a \leq 2\|\tilde{\phi}_j^i\|_a \leq 2D_{K_i}^{\frac{1}{2}} \|\phi_j^i\|_{s(K_i)}.$$

This completes the proof. \square

The above lemma shows the global basis is localizable. We will need one more result before we prove the final convergence estimate, refer to [9].

Lemma 5. *With the same notations in lemma 4, we have*

$$\left\| \sum_{j=1}^{l_i} (\psi_j^i - \psi_{j,\text{ms}}^i) \right\|_a^2 \leq C(k+1)^d \left\| \sum_{j=1}^{l_i} (\psi_j^i - \psi_{j,\text{ms}}^i) \right\|_a^2. \tag{33}$$

Next, we will use the above lemma to estimate of the error between the solution u and the constraint version multiscale solution u_{ms} .

Theorem 1. *Let u be the solution of (2) and u_{ms} be the solution of (19). Define $E = \max_{1 \leq i \leq N_c} E_i$. We have*

$$\|u - u_{\text{ms}}\| \leq C\Lambda_{\Omega^\epsilon}^{-\frac{1}{2}} \|\tilde{\kappa}^{-\frac{1}{2}} f\| + C(k+1)^{\frac{d}{2}} E^{\frac{1}{2}} \|u_{\text{glo}}\|_s,$$

where u_{glo} is the solution of (20). Moreover, if each oversampling parameter k_i is sufficiently large and $\{\chi_i\}_{i=1}^{N_c}$ is a set of bilinear partition of unity, we have

$$\|u - u_{\text{ms}}\|_a \leq CH\Lambda_{\Omega^\epsilon}^{-\frac{1}{2}} \|f\|.$$

Proof. We write $u_{\text{glo}} = \sum_{i=1}^{N_c} \sum_{j=1}^{l_i} c_j^i \psi_j^i$. Subsequently, we express the solution utilizing identical coefficients, but employing local multiscale basis functions, given by $v = \sum_{i=1}^{N_c} \sum_{j=1}^{l_i} c_j^i \psi_{j,\text{ms}}^i \in V_{\text{ms}}$. So, by the Galerkin orthogonality, we have

$$\|u - u_{\text{ms}}\|_a \leq \|u - v\|_a \leq \|u - u_{\text{glo}}\|_a + \left\| \sum_{i=1}^{N_c} \sum_{j=1}^{l_i} c_j^i (\psi_j^i - \psi_{j,\text{ms}}^i) \right\|_a.$$

Recall that the basis functions $\psi_{j,\text{ms}}^i$ have supports in K_{i,k_i} . So, by lemma 4 and lemma 5,

$$\begin{aligned} \left\| \sum_{i=1}^{N_c} \sum_{j=1}^{l_i} c_j^i (\psi_j^i - \psi_{j,\text{ms}}^i) \right\|_a^2 &\leq C(k+1)^d \sum_{i=1}^{N_c} \left\| \sum_{j=1}^{l_i} c_j^i (\psi_j^i - \psi_{j,\text{ms}}^i) \right\|_a^2 \\ &\leq C(k+1)^d \sum_{i=1}^{N_c} E_i \left\| \sum_{j=1}^{l_i} c_j^i \phi_j^i \right\|_s^2 \\ &\leq C(k+1)^d E \|u_{\text{glo}}\|_s^2 \end{aligned}$$

where the last inequality is because $\left\| \sum_{i=1}^{N_c} \sum_{j=1}^{l_i} c_j^i \phi_j^i \right\|_s^2 = \|\pi(u_{\text{glo}})\|_s^2$. By using lemma 2, we obtain

$$\|u - u_{\text{ms}}\|_a \leq C\Lambda_{\Omega^\epsilon}^{-\frac{1}{2}} \|\tilde{\kappa}^{-\frac{1}{2}} f\| + C(k+1)^{\frac{d}{2}} E^{\frac{1}{2}} \|u_{\text{glo}}\|_s.$$

This completes the proof for the first part of the theorem.

To proof the second inequality, we need to estimate the s -norm of the global solution u_{glo} . In particular,

$$\|u_{\text{glo}}\|_s^2 \leq \max\{\tilde{\kappa}\} \|u_{\text{glo}}\|^2 \leq C \max\{\tilde{\kappa}\} \|u_{\text{glo}}\|_a^2.$$

Since u_{glo} satisfies (20), we have

$$\|u_{\text{glo}}\|_a^2 = \int_{\Omega^\epsilon} f u_{\text{glo}} \leq \|\tilde{\kappa}^{-\frac{1}{2}} f\| \|u_{\text{glo}}\|_s.$$

Therefore, we have

$$\|u_{\text{glo}}\|_s \leq C \max\{\tilde{\kappa}\} \|\tilde{\kappa}^{-\frac{1}{2}} f\|.$$

To get the second inequality, we need make $C(k+1)^{\frac{d}{2}} E^{\frac{1}{2}} \max\{\tilde{\kappa}\}$ can be bounded. That is

$$H^{-2} C(k_i+1)^{\frac{d}{2}} E_i^{\frac{1}{2}} = O(1).$$

Taking logarithm,

$$\log(H^{-2}) + \frac{1-k_i}{2} \log\left(1 + \frac{\Lambda_{K_{i,k_i-1}}^{\frac{1}{2}}}{2D_{K_{i,k_i-1}}^{\frac{1}{2}}}\right) + \frac{d}{2} \log(k_i+1) = O(1)$$

That is if we take $k_i = O\left(\log(H^{-1})/\log\left(1 + \Lambda_{K_{i,k_i-1}}^{\frac{1}{2}} \Gamma_{K_{i,k_i-1}}^{-\frac{1}{2}}\right)\right)$ and assume that $\{\chi_i\}_{i=1}^{N_v}$ is a set of bilinear partition of unity, then we have

$$\|u - u_{\text{ms}}\|_a \leq CH\Lambda_{\Omega^\epsilon}^{-\frac{1}{2}} \|f\|.$$

This completes the proof. \square

4.2 Relaxed Version

In this subsection, we will prove the convergence when the multiscale basis functions is in relaxed version. Similar with constraint version, we will prove relaxed version of multiscale basis functions have a decay property first.

The same as the constraint version (lemma 4), we also need to estimate the difference between local multiscale basis functions $\psi_{j,\text{ms}}^i$ and global multiscale basis functions ψ_j^i . We will prove the exponential decay property depends on the oversampling coarse layers k_i and the eigenvalues ratio.

Lemma 6. *Let $\phi_j^i \in V_{\text{aux}}$ be a given auxiliary function. Suppose that $\psi_{j,\text{ms}}^i$ is a multiscale basis function obtained in (14) over the oversampling domain K_{i,k_i} with $k_i \geq 2$ and ψ_j^i is the corresponding global basis function obtained in (17). Then, the following estimate holds:*

$$\|\psi_j^i - \psi_{j,\text{ms}}^i\|_a^2 + \|\pi(\psi_j^i - \psi_{j,\text{ms}}^i)\|_s^2 \leq E_i (\|\psi_j^i\|_a^2 + \|\pi(\psi_j^i)\|_s^2),$$

where $E_i = 3(1 + \Lambda_{\Omega^\epsilon \setminus K_{i,k_i-1}}^{-1}) \left(1 + (2(1 + \Lambda_{K_{i,k_i-1}}^{-\frac{1}{2}}))^{-1}\right)^{1-k_i}$ is a factor of exponential decay.

Proof. By the weak form of $\psi_{j,\text{ms}}^i$ and ψ_j^i in (15) and (18), we have

$$a(\psi_j^i - \psi_{j,\text{ms}}^i, v) + s(\pi(\psi_j^i - \psi_{j,\text{ms}}^i), \pi(v)) = 0, \quad \forall v \in V_0(K_{i,k_i}).$$

Taking $v = w - \psi_{j,\text{ms}}^i$ with $w \in V_0(K_{i,k_i})$ in the above relation, we have

$$\|\psi_j^i - \psi_{j,\text{ms}}^i\|_a^2 + \|\pi(\psi_j^i - \psi_{j,\text{ms}}^i)\|_s^2 \leq \|\psi_j^i - w\|_a^2 + \|\pi(\psi_j^i - w)\|_s^2, \quad \forall w \in V_0(K_{i,k_i}).$$

Let $w = \chi_i^{k_i, k_i-1} \psi_j^i$ in the above relation, we have

$$\|\psi_j^i - \psi_{j,\text{ms}}^i\|_a^2 + \|\pi(\psi_j^i - \psi_{j,\text{ms}}^i)\|_s^2 \leq \|(1 - \chi_i^{k_i, k_i-1})\psi_j^i\|_a^2 + \|\pi((1 - \chi_i^{k_i, k_i-1})\psi_j^i)\|_s^2. \quad (34)$$

From the lemma 1 (iv) and (v), we have

$$\begin{aligned} & \|\psi_j^i - \psi_{j,\text{ms}}^i\|_a^2 + \|\pi(\psi_j^i - \psi_{j,\text{ms}}^i)\|_s^2 \\ & \leq 3(1 + \Lambda_{\Omega^\epsilon \setminus K_{i,k_i-1}}^{-1}) \left(\|\psi_j^i\|_{a(\Omega^\epsilon \setminus K_{i,k_i-1})}^2 + \|\pi(\psi_j^i)\|_{s(\Omega^\epsilon \setminus K_{i,k_i-1})}^2 \right) \end{aligned}$$

Next, we will estimate $\|\psi_j^i\|_{a(\Omega^\epsilon \setminus K_{i,k_i-1})}^2 + \|\pi(\psi_j^i)\|_{s(\Omega^\epsilon \setminus K_{i,k_i-1})}^2$. We will show that this term can be bounded by the term: $\|\psi_j^i\|_{a(\Omega^\epsilon \setminus K_{i,k_i-2})}^2 + \|\pi(\psi_j^i)\|_{s(\Omega^\epsilon \setminus K_{i,k_i-2})}^2$. This recursive property is crucial in our convergence estimate.

Choosing test function $v = (1 - \chi_i^{k_i-1, k_i-2})\psi_j^i$ in (18), we have

$$\begin{aligned} & a(\psi_j^i, (1 - \chi_i^{k_i-1, k_i-2})\psi_j^i) + s(\pi(\psi_j^i), \pi((1 - \chi_i^{k_i-1, k_i-2})\psi_j^i)) \\ & = s(\phi_j^i, \pi((1 - \chi_i^{k_i-1, k_i-2})\psi_j^i)) = 0 \end{aligned} \quad (35)$$

where the last equality follows from the facts that $(1 - \chi_i^{k_i-1, k_i-2})\psi_j^i$ and ϕ_j^i have disjoint support. Note that

$$\begin{aligned}
& a(\psi_j^i, (1 - \chi_i^{k_i-1, k_i-2})\psi_j^i) \\
&= \int_{\Omega^\varepsilon \setminus K_{i, k_i-2}} \nabla \psi_j^i \cdot \nabla ((1 - \chi_i^{k_i-1, k_i-2})\psi_j^i) \\
&= \int_{\Omega^\varepsilon \setminus K_{i, k_i-2}} (1 - \chi_i^{k_i-1, k_i-2}) |\nabla \psi_j^i|^2 - \int_{\Omega^\varepsilon \setminus K_{i, k_i-2}} \psi_j^i \nabla \chi_i^{k_i-1, k_i-2} \cdot \nabla \psi_j^i.
\end{aligned}$$

Consequently, we have

$$\begin{aligned}
\|\psi_j^i\|_{a(\Omega^\varepsilon \setminus K_{i, k_i-1})}^2 &\leq \int_{\Omega^\varepsilon \setminus K_{i, k_i-2}} (1 - \chi_i^{k_i-1, k_i-2}) |\nabla \psi_j^i|^2 \\
&= a(\psi_j^i, (1 - \chi_i^{k_i-1, k_i-2})\psi_j^i) + \int_{\Omega^\varepsilon \setminus K_{i, k_i-2}} \psi_j^i \nabla \chi_i^{k_i-1, k_i-2} \cdot \nabla \psi_j^i. \quad (36) \\
&\leq a(\psi_j^i, (1 - \chi_i^{k_i-1, k_i-2})\psi_j^i) \\
&\quad + \|\psi_j^i\|_{a(K_{i, k_i-1} \setminus K_{i, k_i-2})} \|\psi_j^i\|_{s(K_{i, k_i-1} \setminus K_{i, k_i-2})}.
\end{aligned}$$

Next, from the definition of cutoff function, we can conclude,

$$\begin{aligned}
& s\left(\pi(\psi_j^i), \pi\left((1 - \chi_i^{k_i-1, k_i-2})\psi_j^i\right)\right) \\
&= \|\pi(\psi_j^i)\|_{s(\Omega^\varepsilon \setminus K_{i, k_i-1})} + \int_{K_{i, k_i-1} \setminus K_{i, k_i-2}} \tilde{\kappa} \pi(\psi_j^i) \pi\left((1 - \chi_i^{k_i-1, k_i-2})\psi_j^i\right),
\end{aligned}$$

so we have

$$\begin{aligned}
& \|\pi(\psi_j^i)\|_{s(\Omega^\varepsilon \setminus K_{i, k_i-1})}^2 \\
&= s(\pi(\psi_j^i), \pi\left((1 - \chi_i^{k_i-1, k_i-2})\psi_j^i\right)) - \int_{K_{i, k_i-1} \setminus K_{i, k_i-2}} \tilde{\kappa} \pi(\psi_j^i) \pi\left((1 - \chi_i^{k_i-1, k_i-2})\psi_j^i\right) \quad (37) \\
&\leq s(\pi(\psi_j^i), \pi\left((1 - \chi_i^{k_i-1, k_i-2})\psi_j^i\right)) + \|\psi_j^i\|_{s(K_{i, k_i-1} \setminus K_{i, k_i-2})} \|\pi(\psi_j^i)\|_{s(K_{i, k_i-1} \setminus K_{i, k_i-2})}.
\end{aligned}$$

Finally, summing (36) and (37) and using (35), we have

$$\begin{aligned}
& \|\psi_j^i\|_{a(\Omega^\varepsilon \setminus K_{i, k_i-1})}^2 + \|\pi(\psi_j^i)\|_{s(\Omega^\varepsilon \setminus K_{i, k_i-1})}^2 \\
&\leq \|\psi_j^i\|_{s(K_{i, k_i-1} \setminus K_{i, k_i-2})} \left(\|\psi_j^i\|_{a(K_{i, k_i-1} \setminus K_{i, k_i-2})} + \|\pi(\psi_j^i)\|_{s(K_{i, k_i-1} \setminus K_{i, k_i-2})} \right) \quad (38) \\
&\leq 2(1 + \Lambda_{K_{i, k_i-1} \setminus K_{i, k_i-2}}^{-\frac{1}{2}}) \left(\|\psi_j^i\|_{a(K_{i, k_i-1} \setminus K_{i, k_i-2})}^2 + \|\pi(\psi_j^i)\|_{s(K_{i, k_i-1} \setminus K_{i, k_i-2})}^2 \right)
\end{aligned}$$

where the last inequality follows from lemma 1 (iii). By using this, we have

$$\begin{aligned}
& \|\psi_j^i\|_{a(\Omega^\varepsilon \setminus K_{i, k_i-2})}^2 + \|\pi(\psi_j^i)\|_{s(\Omega^\varepsilon \setminus K_{i, k_i-2})}^2 \\
&= \|\psi_j^i\|_{a(\Omega^\varepsilon \setminus K_{i, k_i-1})}^2 + \|\pi(\psi_j^i)\|_{s(\Omega^\varepsilon \setminus K_{i, k_i-1})}^2 \\
&\quad + \|\psi_j^i\|_{a(K_{i, k_i-1} \setminus K_{i, k_i-2})}^2 + \|\pi(\psi_j^i)\|_{s(K_{i, k_i-1} \setminus K_{i, k_i-2})}^2 \\
&\geq \left(1 + (2(1 + \Lambda_{K_{i, k_i-1} \setminus K_{i, k_i-2}}^{-\frac{1}{2}}))^{-1}\right) \left(\|\psi_j^i\|_{a(\Omega^\varepsilon \setminus K_{i, k_i-1})}^2 + \|\pi(\psi_j^i)\|_{s(\Omega^\varepsilon \setminus K_{i, k_i-1})}^2\right)
\end{aligned}$$

where we used (38) in the last inequality. Using the inequality recursively, we have

$$\begin{aligned} & \|\psi_j^i\|_a^2(\Omega^\epsilon \setminus K_{i,k_i-1}) + \|\pi(\psi_j^i)\|_s^2(\Omega^\epsilon \setminus K_{i,k_i-1}) \\ & \leq \left(1 + (2(1 + \Lambda_{K_{i,k_i-1}}^{-\frac{1}{2}}))^{-1}\right)^{1-k_i} (\|\psi_j^i\|_a^2 + \|\pi(\psi_j^i)\|_s^2). \end{aligned}$$

This completes the proof. \square

Different with the constraint version lemma 6, the above lemma has improved the convergence rate, because the error bound is independent of the constant D . We need the following lemma to prove the convergence, see [10].

Lemma 7. *With the same notation in lemma 6, we have*

$$\begin{aligned} & \left\| \sum_{i=1}^{N_c} \sum_{j=1}^{l_i} c_j^i (\psi_j^i - \psi_{j,ms}^i) \right\|_a^2 + \left\| \sum_{i=1}^{N_c} \sum_{j=1}^{l_i} c_j^i \pi(\psi_j^i - \psi_{j,ms}^i) \right\|_s^2 \\ & \leq C(1 + \Lambda_{\Omega^\epsilon}^{-1})(k+1)^d \sum_{i=1}^{N_c} \left(\left\| \sum_{j=1}^{l_i} c_j^i (\psi_j^i - \psi_{j,ms}^i) \right\|_a^2 + \left\| \sum_{j=1}^{l_i} c_j^i \pi(\psi_j^i - \psi_{j,ms}^i) \right\|_s^2 \right). \end{aligned}$$

Theorem 2. *Let u be the solution of (2) and u_{ms} be the solution of (19). Define $E = \max_{1 \leq i \leq N_c} E_i$. We have*

$$\|u - u_{ms}\| \leq C \Lambda_{\Omega^\epsilon}^{-\frac{1}{2}} \|\tilde{\kappa}^{-\frac{1}{2}} f\| + C(k+1)^{\frac{d}{2}} (1 + \Lambda_{\Omega^\epsilon}^{-1})^{\frac{1}{2}} (1 + D_{\Omega^\epsilon})^{\frac{1}{2}} E^{\frac{1}{2}} \|u_{\text{glo}}\|_s,$$

where u_{glo} is the solution of (20). Moreover, if the oversampling parameter k is sufficiently large and $\{\chi_i\}_{i=1}^{N_v}$ is a set of bilinear partition of unity, we have

$$\|u - u_{ms}\|_a \leq CH \Lambda_{\Omega^\epsilon}^{-\frac{1}{2}} \|f\|.$$

Proof. The proof follows the same procedure as the proof of theorem 1. We write $u_{\text{glo}} = \sum_{i=1}^{N_c} \sum_{j=1}^{l_i} c_{ij} \psi_j^i$ and define $v := \sum_{i=1}^{N_c} \sum_{j=1}^{l_i} c_{ij} \psi_{j,ms}^i$. By the lemma 6 and lemma 7, we have

$$\begin{aligned} \|u_{\text{glo}} - v\|_a^2 & = \left\| \sum_{j=1}^{N_c} \sum_{j=1}^{l_i} c_{ij} (\psi_j^i - \psi_{j,ms}^i) \right\|_a^2 \\ & \leq C(1 + \Lambda_{\Omega^\epsilon}^{-1})(k+1)^d \sum_{i=1}^{N_c} \left(\left\| \sum_{j=1}^{l_i} c_{ij} (\psi_j^i - \psi_{j,ms}^i) \right\|_a^2 + \left\| \sum_{j=1}^{l_i} c_{ij} \pi(\psi_j^i - \psi_{j,ms}^i) \right\|_s^2 \right) \\ & \leq C(1 + \Lambda_{\Omega^\epsilon}^{-1})(k+1)^d \sum_{i=1}^{N_c} E_i \sum_{j=1}^{l_i} (c_{ij})^2 (\|\psi_j^i\|_a^2 + \|\pi(\psi_j^i)\|_s^2). \end{aligned}$$

Choosing the test function $v = \psi_j^i$ in (18), we obtain that $\|\psi_j^i\|_a^2 + \|\pi(\psi_j^i)\|_s^2 \leq \|\phi_j^i\|_s^2 = 1$. Therefore,

$$\begin{aligned}
\|u_{\text{glo}} - v\|_a^2 &\leq C(k+1)^d (1 + \Lambda_{\Omega^\epsilon}^{-1}) (1 + D_{\Omega^\epsilon}) E \sum_{i=1}^{N_c} \sum_{j=1}^{l_i} (c_{ij})^2 \|\phi_j^i\|_s^2 \\
&= C(k+1)^d (1 + \Lambda_{\Omega^\epsilon}^{-1}) (1 + D_{\Omega^\epsilon}) E \sum_{i=1}^{N_c} \sum_{j=1}^{l_i} (c_{ij})^2.
\end{aligned}$$

Next, we will estimate $\sum_{i=1}^{N_c} \sum_{j=1}^{l_i} (c_{ij})^2$. Note that $\pi(u_{\text{glo}}) = \sum_{i=1}^{N_c} \sum_{j=1}^{l_i} c_{ij} \pi(\psi_j^i)$. Using the variational formulation (18), we obtain

$$\begin{aligned}
b_{lk} &:= s(\phi_k^l, \pi(u_{\text{glo}})) \\
&= \sum_{i=1}^{N_c} \sum_{j=1}^{l_i} c_{ij} s(\phi_k^l, \pi(\psi_j^i)) \\
&= \sum_{i=1}^{N_c} \sum_{j=1}^{l_i} c_{ij} (a(\psi_k^l, \psi_j^i) + s(\pi(\psi_k^l), \pi(\psi_j^i)))
\end{aligned}$$

If we denote $a_{ij,lk} := a(\psi_k^l, \psi_j^i) + s(\pi(\psi_k^l), \pi(\psi_j^i)) \in \mathbb{R}^{\mathcal{N} \times \mathcal{N}}$, $\vec{\mathbf{b}} = (b_{lk}) \in \mathbb{R}^{\mathcal{N}}$ and $\vec{\mathbf{c}} = (c_{ij}) \in \mathbb{R}^{\mathcal{N}}$ with $\mathcal{N} := \sum_{i=1}^{N_c} l_i$, then we have

$$\vec{\mathbf{b}} = A \vec{\mathbf{c}} \quad \text{and} \quad \|\vec{\mathbf{c}}\|_2 \leq \|A^{-1}\|_2 \|\vec{\mathbf{b}}\|_2,$$

where $A := (a_{ij,lk}) \in \mathbb{R}^{\mathcal{N} \times \mathcal{N}}$ and $\|\cdot\|_2$ denotes the standard Euclidean norm for vectors in $\mathbb{R}^{\mathcal{N}}$ and its induced matrix norm in $\mathbb{R}^{\mathcal{N} \times \mathcal{N}}$. By the definition of $\pi : V \rightarrow V_{\text{aux}}$, we have

$$\pi(u_{\text{glo}}) = \pi(\pi(u_{\text{glo}})) = \sum_{i=1}^N \sum_{j=1}^{l_i} s(\pi(u_{\text{glo}}), \phi_j^i) \phi_j^i = \sum_{i=1}^N \sum_{j=1}^{l_i} b_{ij} \phi_j^i.$$

Thus, we have $\|\vec{\mathbf{b}}\|_2 = \|\pi(u_{\text{glo}})\|_s$. We define $\phi := \sum_{i=1}^{N_c} \sum_{j=1}^{l_i} c_{ij} \phi_j^i$. Note that $\|\phi\|_s = \|\vec{\mathbf{c}}\|_2$. Consequently, by lemma 3, there exists a function $z \in V$ such that $\pi(z) = \phi$ and $\|z\|_a^2 \leq D_{\Omega^\epsilon} \|\phi\|_s^2$. Since the global multiscale basis ψ_j^i satisfies (18) and u_{glo} is a linear combination of ψ_j^i 's, we have

$$a(u_{\text{glo}}, v) + s(\pi(u_{\text{glo}}), \pi(v)) = s(\phi, \pi(v)) \quad \text{for all } v \in V. \quad (39)$$

Picking $v = z$ in (39), we arrive at

$$\begin{aligned}
\|\phi\|_s^2 &= a(u_{\text{glo}}, z) + s(\pi(u_{\text{glo}}), \pi(z)) \\
&\leq \|u_{\text{glo}}\|_a \cdot D_{\Omega^\epsilon}^{\frac{1}{2}} \|\phi\|_s + \|\pi(u_{\text{glo}})\|_s \cdot \|\phi\|_s \\
&\leq (1 + D_{\Omega^\epsilon})^{\frac{1}{2}} \|\phi\|_s (\|u_{\text{glo}}\|_a^2 + \|\pi(u_{\text{glo}})\|_s^2)^{\frac{1}{2}}.
\end{aligned}$$

Therefore, we have

$$\|\vec{\mathbf{c}}\|_2^2 = \|\phi\|_s^2 \leq (1 + D_{\Omega^\epsilon}) (\|u_{\text{glo}}\|_a^2 + \|\pi(u_{\text{glo}})\|_s^2) = (1 + D_{\Omega^\epsilon}) \vec{\mathbf{c}}^T A \vec{\mathbf{c}}.$$

From the above, we see that the largest eigenvalue of A^{-1} is bounded by $(1 + D_{\Omega^\epsilon})$ and we have the following estimate

$$\|\vec{\mathbf{c}}\|_2 \leq (1 + D_{\Omega^\epsilon}) \|\vec{\mathbf{b}}\|_2 \leq (1 + D_{\Omega^\epsilon}) \|u_{\text{glo}}\|_s.$$

As a result, we have

$$\|u_{\text{glo}} - v\|_a^2 \leq C(k+1)^d (1 + \Lambda_{\Omega^\epsilon}^{-1}) (1 + D_{\Omega^\epsilon}) E (1 + D_{\Omega^\epsilon}) \|u_{\text{glo}}\|_s^2.$$

The rest of the proofs follows from theorem 1. \square

Finally, we remark that all of the main theorem has been proved.

5 Numerical results

In this section, we present two examples using the framework presented in Section 3 for equation (1). The goal is to demonstrate the accuracy of our proposed multiscale model reduction method and establish its linear decrease with the coarse mesh size H when the oversampling layers m are appropriately chosen.

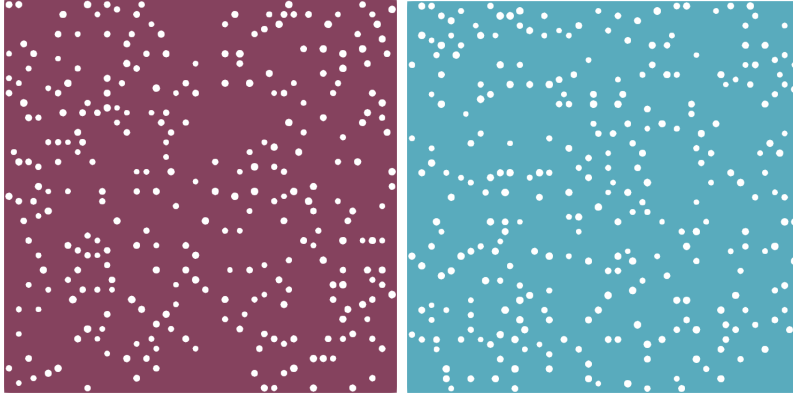


Figure 3: Two heterogenous perforated media used in the simulations. The left media will be used for case 1, while the others will be used for case 2.

In all the examples, we set $\Omega = (0, 1) \times (0, 1)$, and test both constraint version (9) and relaxed version (14). In each case, we will use different media and source term. There are two different perforated domains that depicted in Fig. 3, the left will be test in case 1, while the others in case 2. In this paper, we assume the perforations \mathcal{B}^ϵ are all circular.

In the following experiments, we define some numerical solution errors,

$$e_{L^2} := \frac{\|u_h - u_{\text{ms}}\|}{\|u_h\|}, \quad e_{H^1} := \frac{\|u_h - u_{\text{ms}}\|_a}{\|u_h\|_a}.$$

where u_h is the fine-grid first order FEM solution. In here, we have to note that there are only 3 multiscale basis functions be used in each local domain for every cases.

The computational domains and meshes were constructed using the GMSH software [19]. In each case, fine-grid triangles generated by GMSH had a diameter of $1/200$. To visualize the numerical results, the ParaView software [1] was employed.

5.1 Case 1

In this instance, we employ the perforated domain depicted on the left side of Fig. 3. The source term is illustrated in Fig. 4. Specifically, the source term exhibits only two distinct values within the domain, where we designate four subdomains with a value of 1 (depicted in red) and assign a value of 0 to the remaining regions (depicted in blue).

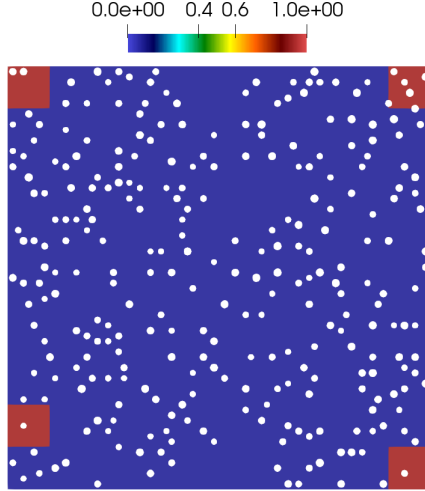


Figure 4: Source term of case 1.

H	m	Constraint Version		Relaxed Version	
		e_{L^2}	e_{H^1}	e_{L^2}	e_{H^1}
1/10	2	4.80e-02	2.04e-01	4.56e-02	2.02e-01
1/20	3	5.72e-03	5.05e-02	5.56e-03	4.98e-02
1/40	4	3.66e-04	6.35e-03	3.50e-04	6.11e-03

Table 1: Numerical errors of CEM-GMsFEM using 3 basis functions in each oversampling domain K_{i,m_i} with different coarse mesh size H . The source and domain are depicted in Fig. 4.

In Table 1, we detail the errors resulting from the refinement of the coarse mesh size alongside appropriately chosen oversampling layers. Both the constraint and relaxed versions of the multi-scale solution demonstrate convergence towards the fine-grid solution, as evidenced by diminishing relative L2 and h1 errors with decreasing H . We further explore the influence of varying oversampling layers while maintaining a constant coarse mesh size H . Figures 5 (constraint version) and 6 (relaxed version) illustrate the errors of the CEM-GMsFEM for varying coarse sizes and oversampling coarse layers. Significantly, these figures highlight the inherent advantage of a linear reduction in error with an increase in coarse mesh size. Additionally, we visually represent the reference solution, constraint oversampling 3 coarse layers (all) diagonal numerical solutions from

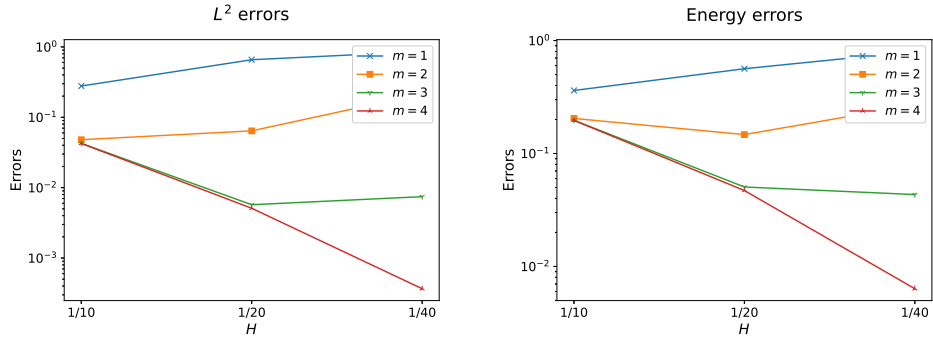


Figure 5: Relative L2 error (Left) and Relative h1 error (Right) of Constraint version of CEM-GMsFEM. In here, we consider case 1, the source term and domain are depicted in Fig. 4.

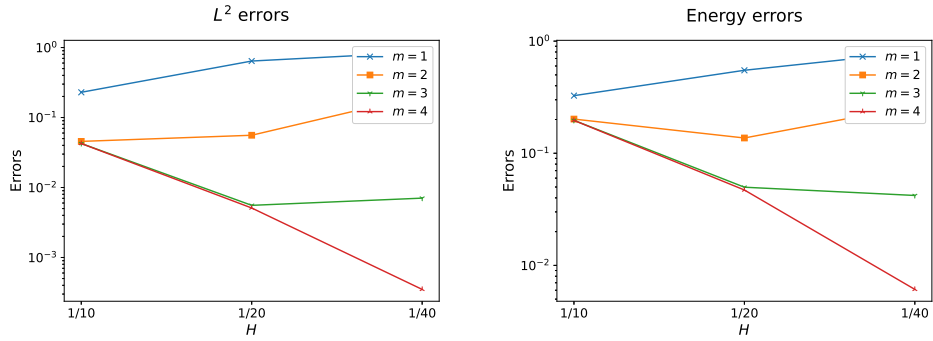


Figure 6: Relative L2 error (Left) and Relative h1 error (Right) of Relaxed version of CEM-GMsFEM. In here, we consider case 1, the source term and domain are depicted in Fig. 4.

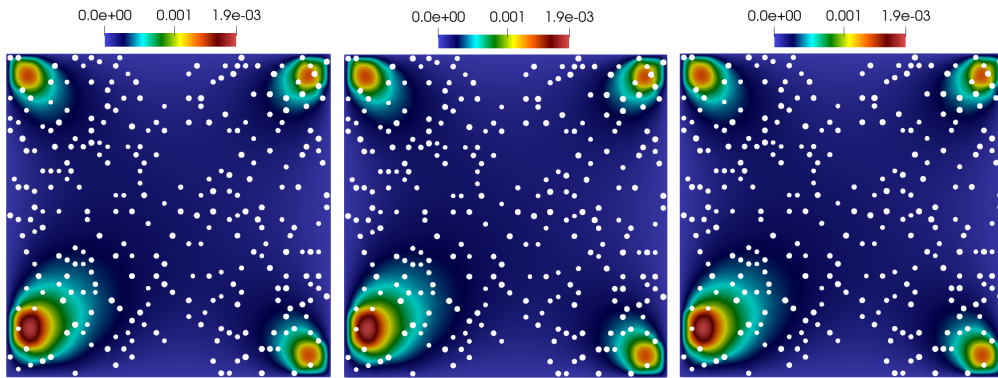


Figure 7: Solutions: Reference solution (top left). Using $H = 1/40$ and oversampling 3 coarse layer, constraint version (top right), relaxed version (bottom). In here, we consider case 1, the source term and domain are depicted in Fig. 4.

Fig. 5 and 6 in Fig. 7. This provides a more vivid example showcasing the diminishing advantage of our method as H decreases.

5.2 Case 2

In this specific scenario, we make use of heterogeneous media showcased on the right side of Fig. 3. The source term is visualized in Fig. 8. Here, the source term is characterized by three distinct values distributed throughout the domain: -1 (depicted in blue), 0 (in green), and 1 (highlighted in red) within specified regions.

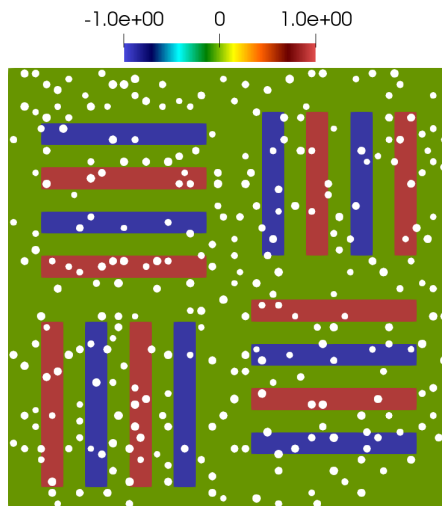


Figure 8: Source term of case 2. There are only three values in the source term, -1 (blue), 0 (green) and 1 (red).

H	m	Constraint Version		Relaxed Version	
		e_{L^2}	e_{H^1}	e_{L^2}	e_{H^1}
1/10	2	2.38e-02	3.60e-02	1.40e-02	2.66e-02
1/20	3	4.77e-03	1.58e-02	3.85e-03	1.40e-02
1/40	4	4.98e-04	5.21e-03	4.68e-04	5.02e-03

Table 2: Numerical errors of CEM-GMsFEM using 3 basis functions in each oversampling domain K_{i,m_i} with different coarse mesh size H . In here, we consider case 2, the source term and domain are depicted in Fig. 8.

In Table 2, we outlines the errors corresponding to the refinement of the coarse mesh size with judiciously chosen oversampling layers. Both the constraint and relaxed versions of the multiscale solution demonstrate convergence toward the fine-grid solution, as evidenced by diminishing relative L2 and h1 errors with decreasing H . Further exploration involves varying oversampling layers

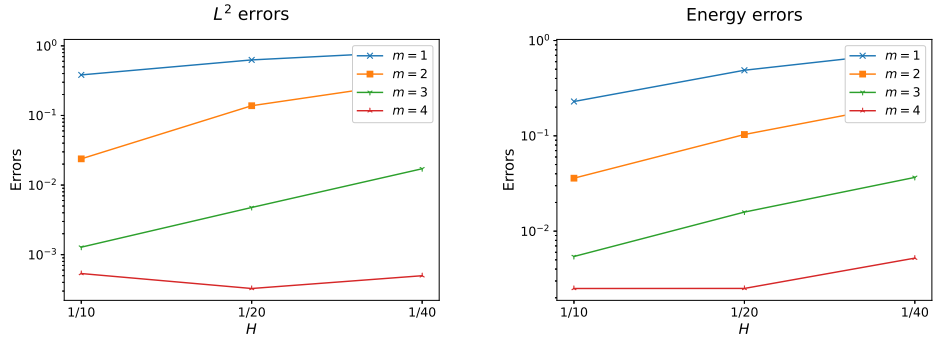


Figure 9: Relative L2 error (Left) and Relative h1 error (Right) of Constraint version of CEM-GMsFEM. In here, we consider case 2, the source term and domain are depicted in Fig. 8.

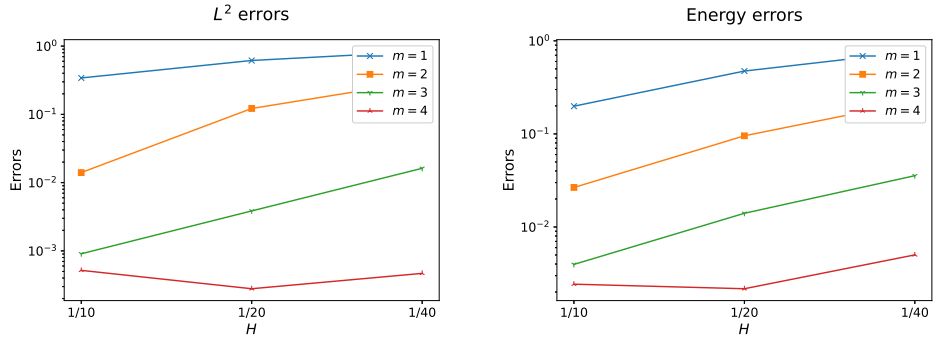


Figure 10: Relative L2 error (Left) and Relative h1 error (Right) of Relaxed version of CEM-GMsFEM. In here, we consider case 2, the source term and domain are depicted in Fig. 8.

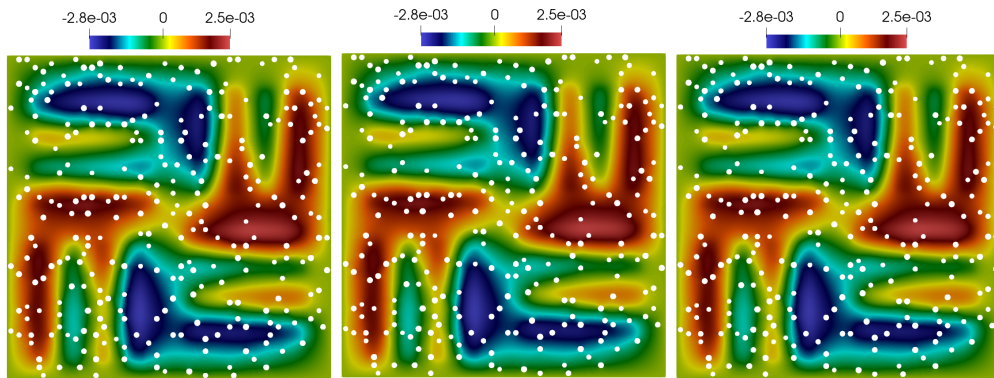


Figure 11: Solutions: Reference solution (top left). Using $H = 1/40$ and oversampling 3 coarse layer, constraint version (top right), relaxed version (bottom). In here, we consider case 2, the source term and domain are depicted in Fig. 8.

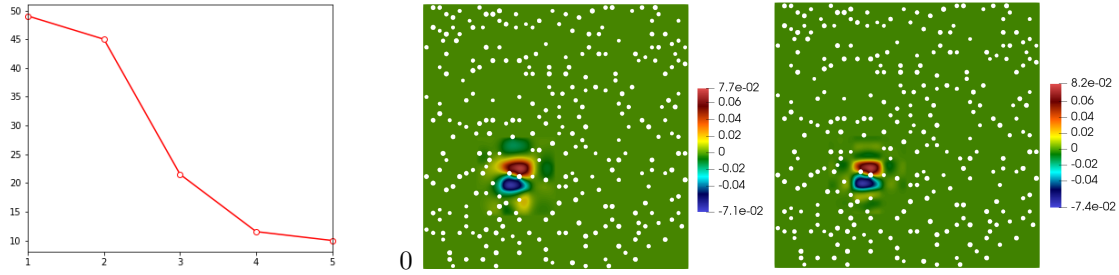


Figure 12: A plot of the inverse of first five nonzero eigenvalues (top left), a multiscale basis function using one nonzero eigenfunction in each local auxiliary space (top right), and a multiscale basis functions using five eigenfunctions in each local auxiliary space (bottom).

while maintaining a constant coarse mesh size H . The errors of the CEM-GMsFEM for distinct coarse sizes and oversampling coarse layers are illustrated in Fig. 9 (constraint version) and 10 (relaxed version). These figures distinctly highlight the advantageous linear reduction in error with increasing coarse mesh size inherent in our proposed approach. To visually underscore these observations, a subset of numerical solutions from Fig. 9 and 10 is selected. The corresponding solutions are depicted in Fig. 11. In Fig. 12, we display the first five nonzero eigenvalues obtained from solving the local spectral problem (8), and a multiscale basis function with one eigenfunction and five eigenfunctions in the local auxiliary space. We can observe that if enough eigenfunctions are exploited in solving the energy minimization problem, then the multiscale basis functions have a fast decay outside of the coarse block.

6 Conclusions

In this study, we introduce and examine a generalized multiscale finite element method designed to minimize constraint energy for solving the Poisson problem in perforated domains. The method initiates by establishing an auxiliary space that employs eigenvectors associated with small eigenvalues in the local spectral problem. Subsequently, leveraging the principles of constraint energy minimization and oversampling, we generate two distinct multiscale basis functions. Our theoretical analysis suggests that with appropriate selection of the oversampling layer, the resulting multiscale basis functions exhibit a decay property. To validate the effectiveness of our approach, we present two numerical experiments.

References

- [1] James Ahrens, Berk Geveci, Charles Law, C Hansen, and C Johnson. 36-paraview: An end-user tool for large-data visualization. *The visualization handbook*, 717:50038–1, 2005.
- [2] Ivo Babuška and Jens M Melenk. The partition of unity method. *International journal for numerical methods in engineering*, 40(4):727–758, 1997.
- [3] Donald L Brown and Daniel Peterseim. A multiscale method for porous microstructures. *Multiscale Modeling & Simulation*, 14(3):1123–1152, 2016.

- [4] Boris Chetverushkin, Eric Chung, Yalchin Efendiev, Sai-Mang Pun, and Zecheng Zhang. Computational multiscale methods for quasi-gas dynamic equations. *Journal of Computational Physics*, 440:110352, 2021.
- [5] Siu Wun Cheung, Eric T Chung, Yalchin Efendiev, and Wing Tat Leung. Explicit and energy-conserving constraint energy minimizing generalized multiscale discontinuous galerkin method for wave propagation in heterogeneous media. *Multiscale Modeling & Simulation*, 19(4):1736–1759, 2021.
- [6] Eric Chung, Yalchin Efendiev, and Thomas Y Hou. Adaptive multiscale model reduction with generalized multiscale finite element methods. *Journal of Computational Physics*, 320:69–95, 2016.
- [7] Eric Chung, Yalchin Efendiev, and Thomas Y Hou. *Multiscale Model Reduction: Multiscale Finite Element Methods and Their Generalizations*. Springer, 2023.
- [8] Eric Chung, Jiuhua Hu, and Sai-Mang Pun. Convergence of the cem-gmsfem for stokes flows in heterogeneous perforated domains. *Journal of Computational and Applied Mathematics*, 389:113327, 2021.
- [9] Eric T Chung, Yalchin Efendiev, and Wing Tat Leung. Constraint energy minimizing generalized multiscale finite element method. *Computer Methods in Applied Mechanics and Engineering*, 339:298–319, 2018.
- [10] Eric T Chung, Yalchin Efendiev, and Wing Tat Leung. Fast online generalized multiscale finite element method using constraint energy minimization. *Journal of Computational Physics*, 355:450–463, 2018.
- [11] Eric T Chung, Yalchin Efendiev, Wing Tat Leung, Maria Vasilyeva, and Yating Wang. Online adaptive local multiscale model reduction for heterogeneous problems in perforated domains. *Applicable Analysis*, 96(12):2002–2031, 2017.
- [12] Eric T Chung, Wing Tat Leung, and Maria Vasilyeva. Mixed gmsfem for second order elliptic problem in perforated domains. *Journal of Computational and Applied Mathematics*, 304:84–99, 2016.
- [13] Eric T Chung, Wing Tat Leung, Maria Vasilyeva, and Yating Wang. Multiscale model reduction for transport and flow problems in perforated domains. *Journal of Computational and Applied Mathematics*, 330:519–535, 2018.
- [14] Eric T Chung, Maria Vasilyeva, and Yating Wang. A conservative local multiscale model reduction technique for stokes flows in heterogeneous perforated domains. *Journal of Computational and Applied Mathematics*, 321:389–405, 2017.
- [15] Yalchin Efendiev, Juan Galvis, and Thomas Y Hou. Generalized multiscale finite element methods (gmsfem). *Journal of computational physics*, 251:116–135, 2013.
- [16] Shubin Fu, Eric Chung, and Tina Mai. Generalized multiscale finite element method for a strain-limiting nonlinear elasticity model. *Journal of Computational and Applied Mathematics*, 359:153–165, 2019.

- [17] Shubin Fu, Eric Chung, and Tina Mai. Constraint energy minimizing generalized multiscale finite element method for nonlinear poroelasticity and elasticity. *Journal of Computational Physics*, 417:109569, 2020.
- [18] Shubin Fu and Eric T Chung. Constraint energy minimizing generalized multiscale finite element method for high-contrast linear elasticity problem. *arXiv preprint arXiv:1809.03726*, 2018.
- [19] Christophe Geuzaine and Jean-François Remacle. Gmsh: A 3-d finite element mesh generator with built-in pre-and post-processing facilities. *International journal for numerical methods in engineering*, 79(11):1309–1331, 2009.
- [20] Patrick Henning and Axel Målqvist. Localized orthogonal decomposition techniques for boundary value problems. *SIAM Journal on Scientific Computing*, 36(4):A1609–A1634, 2014.
- [21] Patrick Henning and Mario Ohlberger. The heterogeneous multiscale finite element method for elliptic homogenization problems in perforated domains. *Numerische Mathematik*, 113:601–629, 2009.
- [22] Matthieu Hillairet. On the homogenization of the stokes problem in a perforated domain. *Archive for Rational Mechanics and Analysis*, 230:1179–1228, 2018.
- [23] Ulrich Hornung. *Homogenization and porous media*, volume 6. Springer Science & Business Media, 1997.
- [24] Thomas Y Hou and Xiao-Hui Wu. A multiscale finite element method for elliptic problems in composite materials and porous media. *Journal of computational physics*, 134(1):169–189, 1997.
- [25] Shan Jiang, Meiling Sun, and Yin Yang. Reduced multiscale computation on adapted grid for the convection-diffusion robin problem. *J. Appl. Anal. Comput*, 7(4):1488–1502, 2017.
- [26] Claude Le Bris, Frédéric Legoll, and Alexei Lozinski. An msfem type approach for perforated domains. *Multiscale Modeling & Simulation*, 12(3):1046–1077, 2014.
- [27] Axel Målqvist and Daniel Peterseim. Localization of elliptic multiscale problems. *Mathematics of Computation*, 83(290):2583–2603, 2014.
- [28] Bagus Putra Muljadi, Jacek Narski, Alexei Lozinski, and Pierre Degond. Nonconforming multiscale finite element method for stokes flows in heterogeneous media. part i: methodologies and numerical experiments. *Multiscale Modeling & Simulation*, 13(4):1146–1172, 2015.
- [29] Aleksei Tyrylgin, Yaoyao Chen, Maria Vasilyeva, and Eric T Chung. Multiscale model reduction for the allen–cahn problem in perforated domains. *Journal of Computational and Applied Mathematics*, 381:113010, 2021.
- [30] Zhongqian Wang, Changqing Ye, and Eric T Chung. A multiscale method for inhomogeneous elastic problems with high contrast coefficients. *Journal of Computational and Applied Mathematics*, 436:115397, 2024.
- [31] E Weinan and Bjorn Engquist. The heterogenous multiscale methods. *Communications in Mathematical Sciences*, 1(1):87–132, 2003.

- [32] Changqing Ye and Eric T Chung. Constraint energy minimizing generalized multiscale finite element method for inhomogeneous boundary value problems with high contrast coefficients. *Multiscale Modeling & Simulation*, 21(1):194–217, 2023.
- [33] GA Yosifian. On some homogenization problems in perforated domains with nonlinear boundary conditions. *Applicable Analysis*, 65(3-4):257–288, 1997.